ORIGINAL PAPER

Influence of lead dioxide surface films on anodic oxidation of a lead alloy under conditions typical of copper electrowinning

T. Nguyen · A. Atrens

Abstract Cyclic voltammograms, current transients at constant potential and potential decay transients have been used to study the formation of lead dioxide surface films in the presence of cobalt ions and their role in decreasing the oxidation rate of a lead alloy under steady state conditions typical of copper electrowinning. The observations in the present work indicate, consistent with the surface film model, that the formation of a continuous $PbSO_4 + \alpha\text{-}PbO_2$ film on the surface of the lead alloy in the presence of cobalt ions hinders further oxidation of the metal. The protectiveness of the film is dynamic in the steady state; the film is continuously forming and dissolving. Also studied was the potential of the oxygen evolution reaction on α-PbO_2 and β-PbO_2 in 170 g L^{-1} H_2SO_4 with and without cobalt ions. The steady state potential for oxygen evolution on β-PbO_2 in 170 g L^{-1} H_2SO_4 at 285 A m^{-2} decreased in the presence of cobalt ions and the steady state potential of β-PbO_2 was essentially the same as that of (i) the Pb–Ca–Sn alloy and (ii) α-PbO_2. The implication is that the potential of the Pb–Ca–Sn alloy is determined by the α-PbO_2 and/or β-PbO_2 on its surface.

Keywords Lead oxidation · Anodic oxidation · Lead anode · Copper electrowinning · Cyclic voltammetry · Oxygen evolution reaction · Lead dioxide

T. Nguyen · A. Atrens (✉)
School of Engineering, The University of Queensland, Brisbane, QLD 4072, Australia
e-mail: a.atrens@minmet.uq.edu.au

1 Introduction

The positive influence of cobalt ions in the electrolyte on the oxidation of lead anodes was first reported in the early 1930s. A small amount of cobalt ions in the electrolyte significantly reduces the oxidation rate of the lead anodes [2, 5, 8, 17, 20]. Our prior work [14, 15] studied the influence of cobalt ions in sulphuric acid on the anodic oxidation of a commercial Pb–Ca–Sn alloy under conditions typical of copper electrowinning using cyclic voltammograms and potential decay transients. The presence of cobalt ions changed the structure, morphology and chemical composition of the surface film, from a loose porous film with a substantial PbO_2 content, to a thin dense film. This change of surface film structure is the cause of the decreased rate of oxidation of the lead anode in the cobalt ion containing solution. The most significant decrease in the lead oxidation rate was for low cobalt ion concentrations (5–25 ppm) so that a significant decrease in lead oxidation rate was evident for cobalt ion concentrations of 50 and 100 ppm. A number of authors [1, 9, 10, 19] have postulated that the reduced potential of the lead anode, in the presence of cobalt ions in the electrowinning solution, results in less lead oxidation. Our prior research [15] showed that the amount of lead oxidized was independent of anodic current density indicating that the mechanisms based on a reduced potential are not applicable to lead oxidation under conditions of electrowinning.

Subsequently, the composition and morphology of the anodic film formed on the lead anode alloy under conditions representative of copper electrowinning was characterized [13] by scanning electron microscopy, X-Ray diffraction (XRD) and X-Ray photoelectron spectroscopy (XPS). No cobalt compounds were detected by XRD and no cobalt peaks were detected by XPS. This indicates that a cobalt film mechanism is not applicable to explain the decreased

oxidation rate in the presence of cobalt ions in sulphuric acid at high current densities. This research indicated that the surface film controls the oxidation rate of the lead alloy. In the presence of a moderate cobalt ion concentration, in steady state there remain the three layers: (i) $PbSO_4$, (ii) α-PbO_2 and (iii) β-PbO_2 in contact with the solution. The presence of cobalt ions improves the imperviousness of the α-PbO_2 in hindering the oxidation of metallic lead to α-PbO_2 and also in hindering the oxidation of $PbSO_4$ to β-PbO_2. In summary, the α-PbO_2 layer is the key to the oxidation rate of the lead alloy.

This paper extends previous [13, 15] to address the following issues: (i) the manner in which the steady state surface film changes with oxidation time, (ii) the influence of cobalt ions on the formation of the initial lead sulphate film, (iii) film formation at constant potential and (iv) the potential of the oxygen evolution reaction on lead dioxide in relation to the oxygen evolution potential on lead anodes. The aim is to more fully understand the mechanism by which cobalt ions decrease the oxidation of the lead alloy under steady state conditions typical of copper electrowinning.

2 Experimental

2.1 Electrochemical cell

The water-jacketed glass three-electrode electrochemical cell had a volume of 200 mL. The electric motor for the rotating working electrode was mounted directly above the cell. A Luggin capillary was fitted in the bottom of the cell via a threaded port. A platinum wire was used as the counter electrode. Unless otherwise stated, the electrolyte was a 170 g L^{-1} H_2SO_4 solution. The cobalt ions were added to the solution in the form of cobalt sulphate, $CoSO_4 \cdot 7H_2O$. All solutions were prepared with AR grade chemicals and distilled water. A Hg|HgSO$_4$|saturated K_2SO_4 reference electrode was used to avoid chloride contamination. The potentials are reported with respect to the standard hydrogen electrode (SHE). The potential of the working electrode was controlled by a PAR 362 scanning potentiostat. The potential and current from the potentiostat were logged by a computer using a data acquisition system operated by Lab VIEW 7 software. All measurements were made at room temperature.

2.2 Anodic oxidation of the lead alloy

The working electrode was a rotating disc in the shape of a cylinder attached to a stainless steel disc using conductive silver-loaded epoxy and embedded in epoxy resin (Araldite LC 191, Hardener LC 26). The composition of the

commercial Pb–Ca–Sn alloy was 1.4%Sn, 0.080%Ca, 0.020%Al and balance Pb. Unless stated otherwise, the electrode was rotated at 500 rpm. Immediately before each experiment, the electrode was polished using 1200-grit paper and thoroughly rinsed with acetone and distilled water.

2.3 Oxygen evolution on lead dioxide

The PbO_2 deposits were prepared on a substrate of platinum (Pt) or vitreous carbon. Prior to the deposition, each substrate was gently roughened with sand paper to increase the adhesion of the PbO_2 deposit; polarised in a 10% sodium hydroxide solution for 30 min with a 1 mA anodic current in the electrochemical cell to remove any particles on the surface; immersed in a 10% nitric acid solution for 10 min and thoroughly washed with distilled water.

The deposits of β-PbO_2 and α-PbO_2 were produced by anodic electrodeposition as described by Narasimham and Udupa [12] and Devilliers et al. [4] in a water-jacketed cell on either vitreous carbon or Pt, 2.95 mm or 2 mm in diameter, with an exposed surface area of 6.83×10^{-6} m^2 and 3.14×10^{-6} m^2 respectively. A stainless steel plate was used as the cathode. All chemicals were AR reagents. The crystallographic form of the PbO_2 deposit was characterised by X-ray diffraction (XRD).

Pure β-PbO_2 was electrodeposited from an electrolyte containing 350 g L^{-1} lead nitrate ($Pb(NO_3)_2$) and 30 g L^{-1} copper nitrate ($Cu(NO_3)_2$) at a current density of 300 A m^{-2} at 65 °C for 5 min. The copper ions prevented the deposition of dendritic lead on the cathode, which would decrease the efficiency of PbO_2 deposition on the anode. Copper, being more electropositive than lead, deposits preferentially on the cathode.

Pure α-PbO_2 was deposited from 140 g L^{-1} NaOH and 50 g L^{-1} PbO with a current density of 10 A m^{-2} for 2 h at 30 °C.

Each PbO_2 electrode was removed from the plating solution, carefully rinsed in distilled water, introduced into the 170 g L^{-1} H_2SO_4 solution containing the required cobalt concentration and oxidised for a specified time at a rotation rate of 500 rpm and at a constant current density of 285 A m^{-2}. The PbO_2 electrodes were examined using scanning electron microscopy (SEM) and X-ray diffraction (XRD) before and after oxidation.

3 Results and discussion

3.1 Anodic oxidation of lead anode at constant current

A typical cyclic voltammogram is presented in Fig. 1. This was measured after the Pb–Ca–Sn alloy had been oxidised
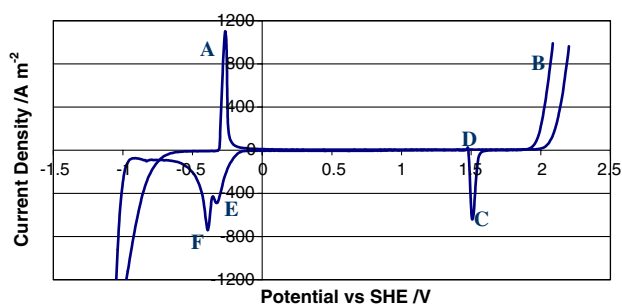
Fig. 1 Typical cyclic voltammogram, at room temperature and at 500 rpm, of a rotating Pb–Ca–Sn alloy electrode after 24 h oxidation at 285 A m^{-2} in 170 g L^{-1} H$_2$SO$_4$. The potential was swept at 10 mV s^{-1} in a negative direction from the potential at ∼2.1 V. Subsequently the positive scan was measured

Fig. 2 The influence of the cobalt ion concentration on the potential of the Pb–Ca–Sn alloy during oxidation at 285 A m^{-2}. The potential approached steady state during the first hour as plotted. There was no substantial change during the remainder of the 24 h period of oxidation (not plotted)

for 24 h at 285 A m^{-2} in 170 g L^{-1} H$_2$SO$_4$ and PbO, PbO$_2$ and PbSO$_4$ had formed on the surface during this oxidation. The voltammogram was measured at a scan rate of 10 mV s^{-1}, a scan rate not untypical for such research. The potential during the oxidation was ∼2.1 V. During the negative scan from this potential, reduction of PbO$_2$ to PbSO$_4$ occurs at about 1.55 V (peak C), followed by a small anodic peak D at about 1.45 V, the reduction of PbO to Pb at about −0.4 V (peak E), PbSO$_4$ to Pb at −0.45 V (peak F) and the evolution of hydrogen at more negative potentials. The small peak D is generally interpreted as being due to the oxidation of metallic lead to lead sulphate or oxide [3, 16] in cracks produced in the PbO$_2$ film during reduction to lead sulphate. On the positive scan from negative potentials, the oxidation of Pb to PbSO$_4$ occurs at approximately −0.3 V.

The quantity of Pb oxidised to PbO$_2$ during the anodic oxidation can be evaluated by integrating the charge under peak C whilst the total amount of Pb oxidised can be obtained from the area under peaks E and F. This method of evaluation of the oxidation rate assumes that all the oxidation products remain on the electrode surface during oxidation. After each experiment the solution was carefully examined and there was no evidence of spalling of oxidation products. The oxidation rate is presented in terms of the total mass of Pb oxidised in terms of the equation

$$W = \frac{MIt}{nF} \tag{1}$$

where W = weight of the electro-active species/g, M = molecular mass of lead, I = current/A, t = time/s and F = Faraday = 96480 C mol^{-1}. The oxidation rate is conventionally expressed in units of g Pb (kAh)$^{-1}$.

Figure 2 shows the potential of the Pb–Ca–Sn alloy during oxidisation at a constant current density of 285 A m^{-2}. In agreement with [15], the steady state potential of the Pb–Ca–Sn alloy decreased with increasing
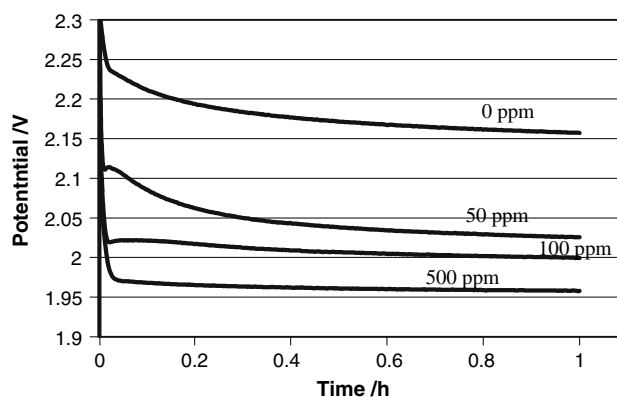
cobalt ion concentration. The steady state potential decreased approximately 197 mV in the presence of 500 ppm Co^{2+}. The progressive decrease in potential with increasing [Co^{2+}] indicates a progressive facilitation of oxygen evolution.

The extent of oxidation of the Pb–Ca–Sn alloy, expressed as the amount of PbO$_2$ and total Pb oxidised, derived from the voltammograms measured after 24 h oxidation for the experiments shown in Fig. 2 are summarised in Fig. 3. These results are in agreement with [15]. Both the amount of PbO$_2$ and the total oxidation rate decreased with increasing cobalt ion concentration. The largest decrease occurred for small cobalt ion concentrations, concentrations less than 20 ppm.

Figure 4 shows that the oxidation rate decreased steadily from the values measured after 1 h oxidation until steady state had been reached by 24 h of oxidation. The values measured in this work after 1 h oxidation were consistent
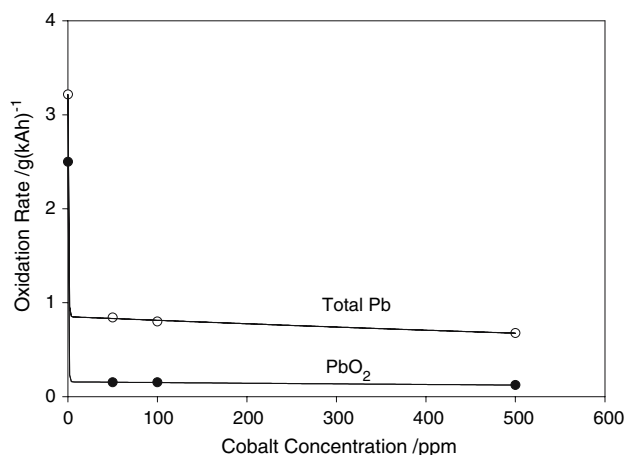

Fig. 3 The influence of cobalt ion concentration on the oxidation rate (expressed as total Pb) and the amount of PbO$_2$ (expressed as Pb) of the Pb–Ca–Sn alloy oxidised for 24 h at 285 A m^{-2}
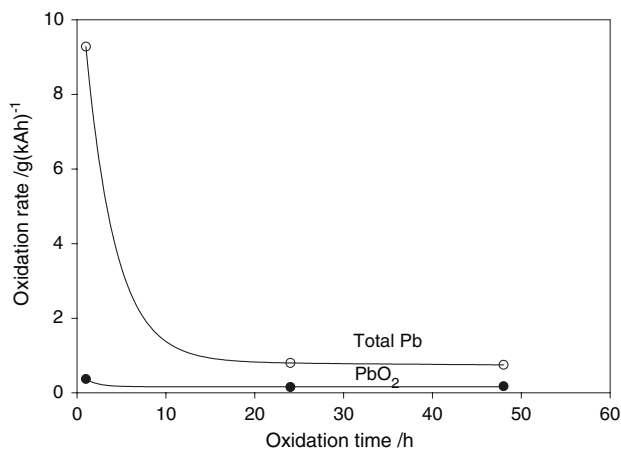
Fig. 4 Time dependence of the oxidation rate for the Pb–Ca–Sn alloy in 170 g L^{-1} H$_2$SO$_4$ + 100 ppm Co^{2+}

with the values measured [15] indicating consistency of the present study with [15]. The oxidation rate of 1 gPb (kAh)$^{-1}$ is equivalent to a fraction of 6.6×10^{-4} of the available electrons being used in the oxidation of the lead alloy, the remainder being used in the evolution of oxygen.

Figure 5 presents scanning electron microscope (SEM) micrographs of the film formed on the anode surface after 24 h oxidation in 170 g L^{-1} H$_2$SO$_4$ with 0 ppm and 500 ppm cobalt. The anodic film formed in the cobalt-free solution was thick and porous whereas the film was compact when formed in the presence of 500 ppm Co^{2+}. These observations indicate that, consistent with [15], the formation of a continuous surface film in the presence of cobalt ions hinders further oxidation of the metal. The film formed in the presence of 500 ppm (and 24 h oxidation) was significantly more compact than films formed under comparable cobalt concentrations (1 h oxidation) [15]. The more compact film formed in the presence of the 500 ppm (and 24 h oxidation) and the considerably lower oxidation rate under steady state conditions, as shown in Fig. 4, indicate that the protectiveness of the film is a dynamic effect; i.e., the film is continuously forming and dissolving.
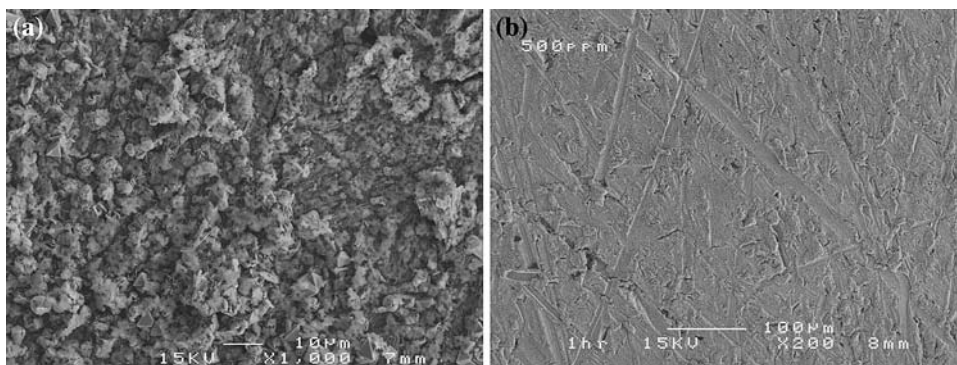
Hrussanova et al. [8] speculated that the porous film consisted of β-PbO$_2$; the dense part was composed of PbO$_t$, PbO$_x$ and α-PbO$_2$; and that the oxidation rate increased with the content of β-PbO$_2$ in the anodic film. Our previous work [13] indicated that a continuous α-PbO$_2$ layer was the key factor in determining the oxidation rate. The presence of cobalt ions improves the imperviousness of the α-PbO$_2$ in hindering the oxidation of metallic lead to α-PbO$_2$ and also in hindering the oxidation of PbSO$_4$ to β-PbO$_2$.

Figure 6 presents the cathodic branch of the cyclic voltammogram for the Pb–Ca–Sn alloy after oxidation for 24 h in 170 g L^{-1} H$_2$SO$_4$ solution. For moderate Co^{2+} ion concentrations, Fig. 6a, there is a clear peak C associated with lead dioxide. At much higher concentrations of 5000 ppm, Fig. 6b, there was no trace of the cathodic peak C at 1.5 V corresponding to the reduction of PbO$_2$ to PbSO$_4$. The quality of PbO$_2$ formed was not detectable by the cyclic voltammogram technique. The cathodic peaks at approximately −0.25 to −0.35 V (representing the reductions of PbO to Pb and PbSO$_4$ to Pb) indicated that PbO and PbSO$_4$ were the main products of oxidation at this high cobalt concentration.

Figure 7 presents the subsequent anodic branch measured for potentials −0.5 to −0.1 V. The peak height corresponding to the oxidation of Pb to PbSO$_4$ decreased progressively with increase in Co^{2+} concentration. This decreasing amount of PbSO$_4$ was observed previously [15], but contradicts the results of Ramachandran and Balakrishnan [18].

3.2 Voltammograms of freshly polished Pb–Ca–Sn alloy electrodes

Figure 8 shows voltammograms for the Pb–Ca–Sn alloy scanned at a scan rate of 5 mV s^{-1} from 1.4 to 2.2 V in four different solutions. The two anodic peaks are designated as B1 and B2 [5–8, 11, 20, 21]. The anodic peak B1, at 1.6–1.7 V, is attributed to the oxidation to produce α-PbO$_2$ from a range of possible starting compounds such

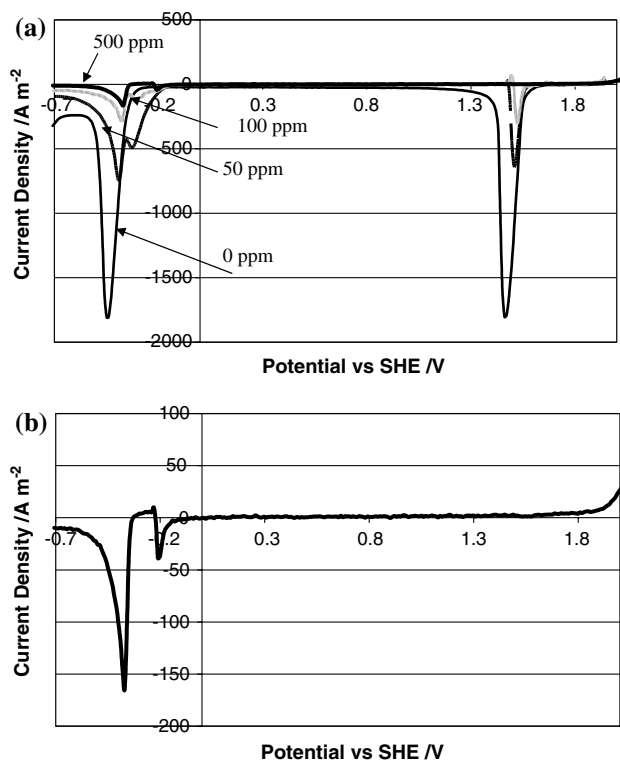**Fig. 5** SEM micrographs of the anodic film on the Pb–Ca–Sn alloy after 24 h oxidation at 285 A m^{-2} and 500 rpm at room temperature (**a**) 170 g L^{-1} H$_2$SO$_4$, (**b**) 170 g L^{-1} H$_2$SO$_4$ + 500 ppm Co^{2+}

Fig. 6 Cyclic voltammogram for the Pb–Ca–Sn alloy oxidised for 24 h in 170 g L^{-1} H$_2$SO$_4$ and (**a**) 0 to 500 ppm Co^{2+} and (**b**) 5000 ppm Co^{2+}
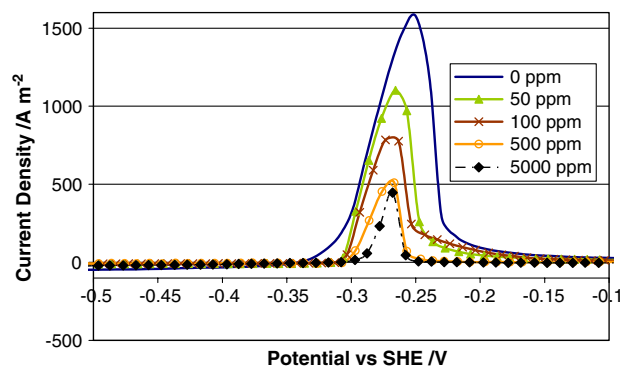

Fig. 7 Anodic potential sweep of the voltammogram for the Pb–Ca–Sn alloy in 170 g L^{-1} H$_2$SO$_4$ and stated cobalt concentration in the potential range −0.5 to −0.1 V at 10 mV s^{-1} and 500 rpm

as $xPbO \cdot PbSO_4$, PbO or Pb [11, 20–22]. The anodic peak B2, at 1.85–1.9 V, is attributed to the oxidation of PbSO$_4$ to β-PbO$_2$ [5, 8, 20].

For a cobalt ion concentration of 0 mg L^{-1}, peaks B1 and B2 were significant in size; that indicates a significant amount of current was used in the production of lead dioxide which is consistent with a thick and discontinuous surface layer as presented in Fig. 5. At potentials above 2.0 V, the current increased rapidly with increasing
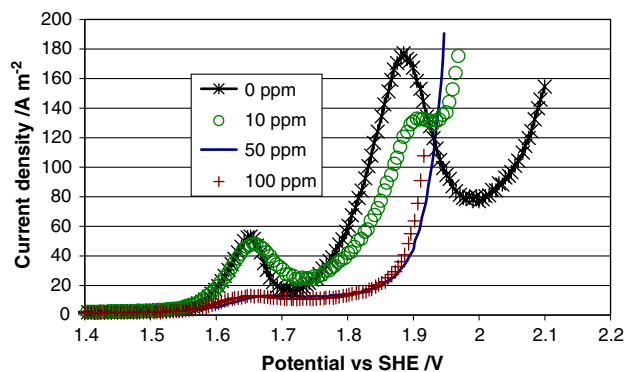

Fig. 8 Anodic scan of the voltammogram for the freshly polished Pb–Ca–Sn alloy at scan rate 5 mV s^{-1} in 170 g L^{-1} H$_2$SO$_4$ solution with the stated cobalt concentrations

potential; this is attributed to the oxygen evolution reaction.

For a cobalt ion concentration of 10 mg L^{-1}: (i) the peak B1 shifted marginally to a somewhat higher potential and was somewhat broader (indicative of the production of a comparable amount of α-PbO$_2$); (ii) the peak B2 was significantly smaller (indicative of the production of a much smaller amount of β-PbO$_2$ consistent with Fig. 3), and (iii) the oxygen evolution reaction became evident at much lower values of potential (which is consistent with Fig. 2). It is interesting that the potential for peak B2 shifted to a more positive value as the cobalt ion concentration increased from 0 to 10 ppm, which suggests that at higher cobalt ion concentrations the energy barrier is higher for the formation of β-PbO$_2$ from PbSO$_4$, thereby inhibiting the oxidation of PbSO$_4$ to β-PbO$_2$. The relative peak heights for peaks B1 and B2 are given in Table 1.

For cobalt ion concentrations of 50 and 100 mg L^{-1}: (i) the peak B1 was much smaller and had also shifted to a somewhat higher potential (indicative of the production of a significantly smaller amount of α-PbO$_2$, the amount produced being similar at these two cobalt ion concentrations); (ii) the peak B2 was absent (indicative of the production of a negligible amount of β-PbO$_2$ consistent with Fig. 3), and (iii) the oxygen evolution reaction became evident at increasingly lower values of potential (which is consistent with Fig. 2).

The surface film on the lead alloy for the various cobalt concentrations can be understood in terms of layers of

Table 1 Relative peak heights for peaks B1 and B2 in Fig. 7

Co^{2+} (ppm)	Peak B1, α-PbO$_2$	Peak B2, β-PbO$_2$
0	57	160
10	55	55
50	17	0
100	17	0

PbSO$_4$, α-PbO$_2$ and β-PbO$_2$, where the relative amounts of the two forms of lead dioxide are given by the relative peak heights for peaks B1 and B2, Table 1. The film becomes thinner and with much less β-PbO$_2$ as the cobalt ion concentration is increased from 0 to 10 and 50 ppm. This correlated with the decreased rate of oxidation of the lead alloy, as given in Fig. 3. This is consistent with the surface film model, which indicates that the α-PbO$_2$ layer is the key to the oxidation rate of the lead alloy [13].

3.3 Oxidation of the lead alloy at constant potential

A typical current-time transient is shown in Fig. 9 for the freshly polished Pb–Ca–Sn alloy whilst it was oxidized at a constant potential of 1.9 V for 24 h in 170 g L^{-1} H$_2$SO$_4$ solution. The current (i) increased then decreased as the sulphate layer was formed, (ii) increased to a plateau due to the formation of lead dioxide and (ii) continued to rise until it reached a nearly constant value (attributed to oxygen evolution) after 10–20 h with only a very slight decrease in current from then on. Only the first 3 h are shown in the figure. The current-time transients at 1.85, 1.9 and 1.95 V are presented in Fig. 10a–c.

At V = 1.85 V (Fig. 10a), the curves exhibited a significant initial transient consistent with the production of a surface film of significant thickness containing lead sulphate and lead dioxide consistent with the data of Figs. 3, 5 and 6. The steady state current values were low, which indicated that the amount oxygen evolution was limited at this potential. The steady state current was higher in the presence of cobalt ions in solution, consistent with Fig. 8, indicating that cobalt ions facilitate the oxygen evolution reaction. Nevertheless, the oxygen evolution rate was increased by only ~ 7 A m^{-2} for 1000 ppm Co^{2+} in the solution. At V = 1.9 V, the steady state current density for

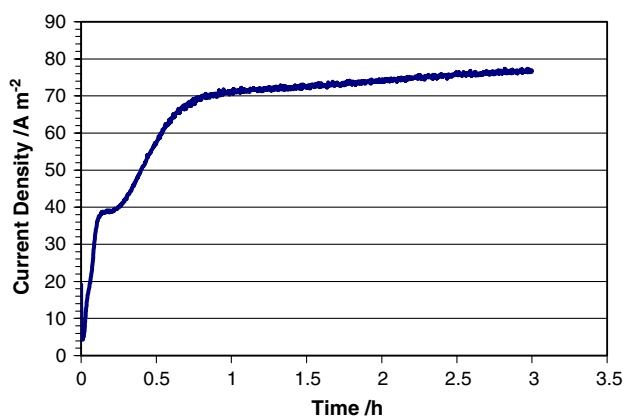Fig. 9 Typical current-time transient for the Pb–Ca–Sn alloy during oxidisation at 1.9 V in 170 g L^{-1} H$_2$SO$_4$ containing 1000 ppm Co^{2+} at room temperature and 500 rpm
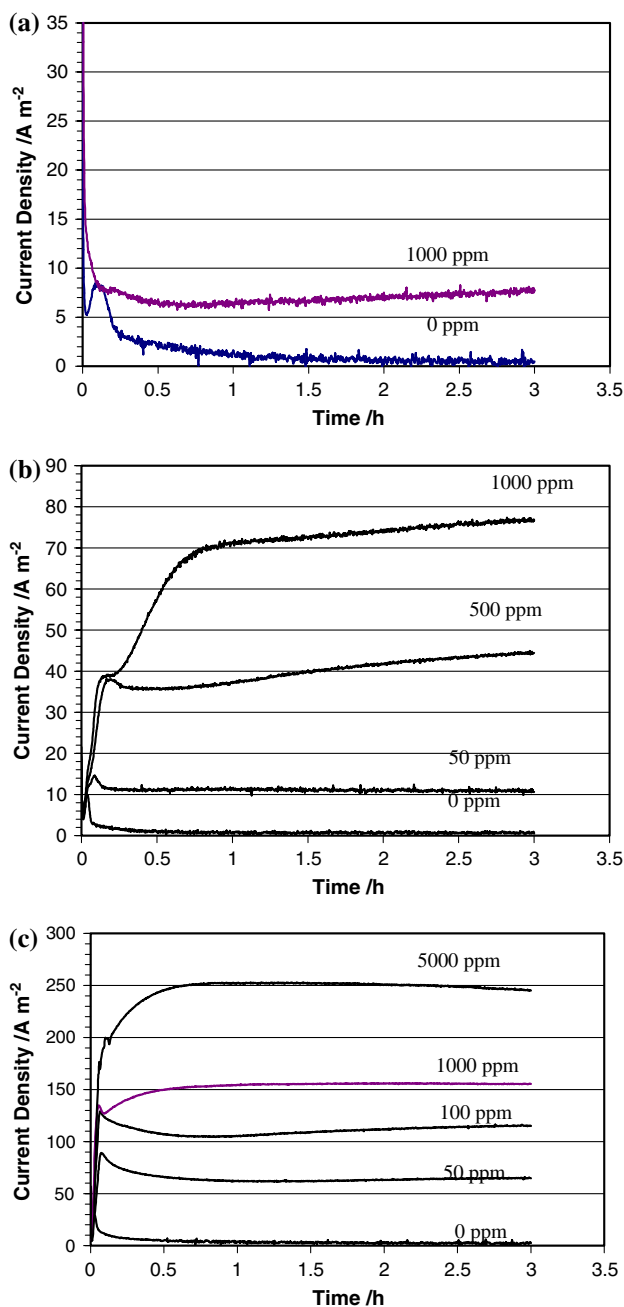

Fig. 10 Influence of cobalt ion concentration on the current/time curves for the Pb–Ca–Sn alloy oxidized at constant potential at (a) 1.85 V, (b) 1.9 V and (c) 1.95 V

oxygen evolution increased by ten fold compared to that at 1.85 V. At V = 1.95 V, the effect of cobalt on oxygen evolution was even more pronounced with a current density of about 60 A m^{-2} with just 50 ppm Co^{2+}. These results showed that the evolution of oxygen was enhanced at potentials above 1.9 V.

Figure 11 presents plots of the steady state current versus potential (from Fig. 10) for the Pb–Ca–Sn alloy oxidised at constant potential. Comparison with Fig. 8
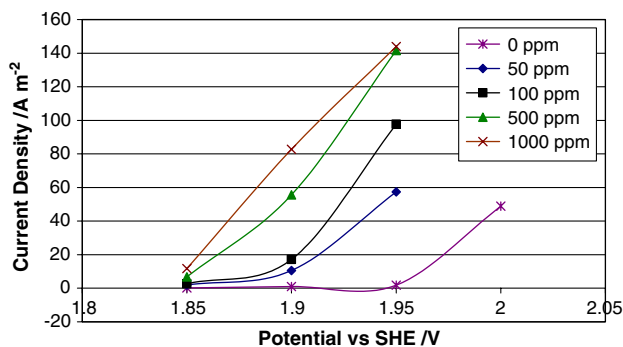
Fig. 11 Plots of steady state current (from Fig. 10) for the Pb–Ca–Sn alloy oxidized at constant potential

indicates that the peaks B1 and B2 are absent in the steady state. This again indicates that the formation of the lead dioxide surface film is a transient phenomenon.

3.4 Potential decay transients

The formation of lead compounds was examined by means of potential decay transients for the lead alloy oxidised at 1.85, 1.9 and 1.95 V, Fig. 12. The potential remained for some time period at a potential plateau corresponding to the presence of lead dioxide, then decreased rapidly to the $PbSO_4$ potential. The times at the plateau are presented in Table 2; assuming that the form of the lead dioxide is the same in all cases and that its ease of reduction is the same, then the time at the lead dioxide plateau give an indication of the amount of lead dioxide formed.

For the lead alloy oxidised at 1.95 V, the amount of surface lead dioxide decreased significantly with increasing cobalt ion concentration; from that corresponding to a lead dioxide plateau of 4.8 min for a cobalt ion concentration of 0 ppm decreasing to 0.4 min for a cobalt ion concentration of 500 ppm. This trend is consistent with that observed in the voltammograms (Fig. 3) and from the surface observations (Fig. 5).

For the lead alloy oxidised at the lower voltages of 1.85 and 1.9 V, there was no correlation between the amount of lead dioxide and the cobalt ion concentration. This implies that the modification of the surface film by the cobalt ions requires the potential to be at 1.95 V or above.

3.5 Oxygen evolution on PbO_2

For the β-PbO_2 electrodeposited on vitreous carbon, XRD confirmed that the electrodeposit contained mainly β-PbO_2. The potential for oxygen evolution on the β-PbO_2 in 170 g L^{-1} H_2SO_4 at 285 A m^{-2} at the stated cobalt
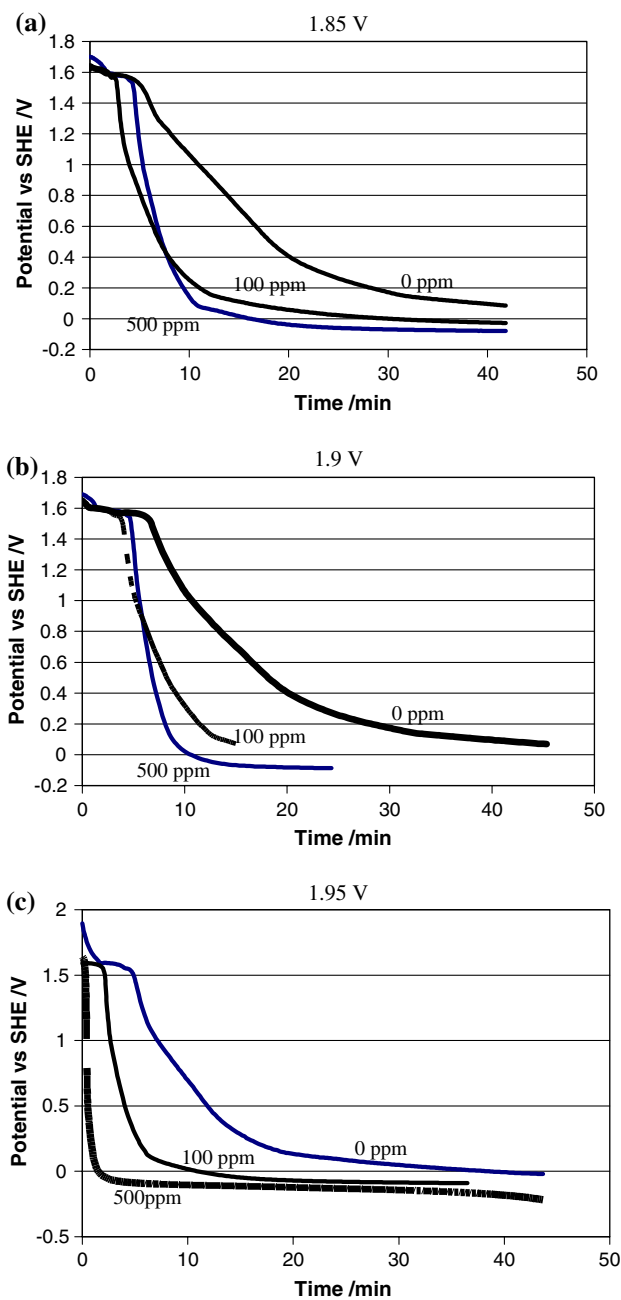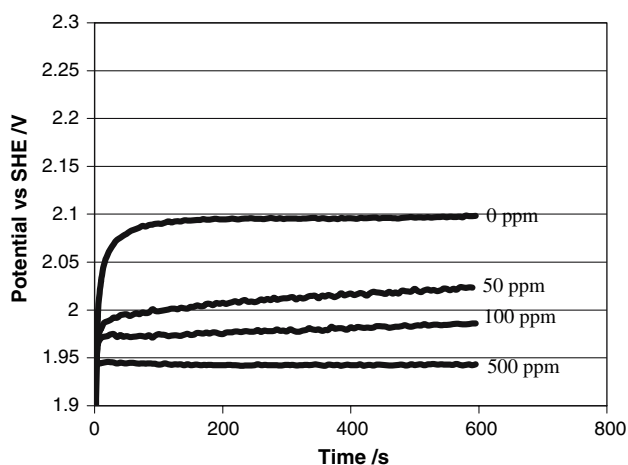

Fig. 12 Potential of the Pb–Ca–Sn alloys after 24 h oxidation at constant potential at (**a**) 1.85 V, (**b**) 1.9 V and (**c**) 1.95 V

concentrations is shown in Fig. 13. The steady state potential was reduced in the presence of the cobalt ions in the solution. The steady state potential of β-PbO_2 was essentially the same as the potential of the Pb–Ca–Sn alloy measured in [15] and also as measured in this work, Fig. 2. About 500 ppm Co^{2+} decreased the potential of Pb–Ca–Sn by 190 mV whilst the potential of β-PbO_2 was reduced by 155 mV. About 100 ppm and 50 ppm Co^{2+} reduced the potential of Pb–Ca–Sn by 136 and 115 mV whilst the potential of β-PbO_2 was reduced by 112 and 74 mV,

Table 2 The times at the plateau corresponding to lead dioxide

Cobalt concentration/ ppm	Duration of potential of lead alloy at lead dioxide plateau/min		
	1.85 V	1.90 V	1.95 V
0	4.3	2.0	4.8
100	2.9	1.8	1.8
500	4.3	3.2	0.4

Fig. 13 Effect of cobalt ion concentration on the potential of β-PbO$_2$

respectively. The implication is that the potential of the Pb–Ca–Sn alloy is determined by the β-PbO$_2$ on its surface as determined in [15].

Subsequently the potentials were measured for α-PbO$_2$ and β-PbO$_2$ electrodeposited on Pt. The potential, in 170 g L^{-1} H$_2$SO$_4$ at 285 A m^{-2} at a cobalt ion concentration of 100 ppm, of α-PbO$_2$ and β-PbO$_2$ was essentially the same. The potential of β-PbO$_2$ remained essentially unchanged and essentially equal to that presented in Fig. 2. The potential of α-PbO$_2$ had a slight increase and reached almost 2.0 V after 24 h.

Figure 13 showed that the steady state potential for oxygen evolution on β-PbO$_2$ in 170 g L^{-1} H$_2$SO$_4$ at 285 A m^{-2} was decreased in the presence of cobalt ions, and moreover the steady state potential of β-PbO$_2$ was essentially the same as the potential of the Pb–Ca–Sn alloy measured in Fig. 2 and in [15]. The steady state potential for oxygen evolution of α-PbO$_2$ in 170 g L^{-1} H$_2$SO$_4$ at 285 A m^{-2} was initially essentially the same as that of β-PbO$_2$. The implication is that the potential of the Pb–Ca–Sn alloy is determined by the α-PbO$_2$ and/or β-PbO$_2$ on its surface and that the lead dioxide catalyses the oxygen evolution reaction when the lead dioxide surface layer is formed in the present of cobalt ions. This is consistent with the suggestion by Cachet et al. [2] that

Co^{2+} ions alter the catalytic properties of the active centres involved in the oxygen evolution reaction. Thus the influence of the cobalt ions in solution is quite subtle. It is an indirect influence, in that the influence is to change the surface film, from a thick porous film to a thin compact film. Moreover, the catalytic properties are enhanced, so that the oxygen evolution reaction is facilitated. The film on the lead surface is more compact and more protective. The film is also more catalytic in facilitating the oxygen evolution reaction. This second film property (catalytic) is useful commercially (decreases costs) however it appears not to be directly related to the increased oxidation resistance, because, [15] showed that the lead oxidation was not related to potential.

4 Conclusions

- In the presence of cobalt ions in the electrolyte, the potential of the lead alloy decreased, as did the amount of surface corrosion product.
- The oxidation rate in the presence of cobalt ions decreases significantly with increasing oxidation time to a steady state value, indicating that the protectiveness of the surface film is dynamic, the film is continuously forming and dissolving.
- The surface film in the absence of cobalt ions was thick and porous, whereas the film was thin and compact when formed in the presence of cobalt ions.
- The present study indicates, consistent with the surface film model, that the formation of a continuous PbSO$_4$ + α-PbO$_2$ film on the surface of the lead alloy in the presence of cobalt ions hinders further oxidation of the metal. The protectiveness of the film is dynamic; the film is continuously forming and dissolving.
- The presence of cobalt in the solution decreases the amount of PbSO$_4$ formed on the alloy surface.
- The lead dioxides α-PbO$_2$ and β-PbO$_2$ form in the potential region above about 1.55 V.
- Potential decay transients after oxidation at constant potential indicated that the influence of cobalt ions on the lead dioxide occurred for potentials of 1.95 V and above.
- Measurement of the potential of the oxygen evolution reaction on α-PbO$_2$ and β-PbO$_2$ in 170 g L^{-1} H$_2$SO$_4$ with and without cobalt ions in the solution indicated that the potential of the Pb–Ca–Sn alloy is determined by the α-PbO$_2$ and/or β-PbO$_2$ on its surface and that the lead dioxide catalyses the oxygen evolution reaction.

577

References

1. Antonov SP, Stepanenko VG (1972) Ukrainskii Khimicheskii Zhurnal 38:935
2. Cachet C, Pape-rérolle C Le, Wiart R (1999) J Appl Electrochem 29:811
3. Czerwinski A, Zelazowska M, Grden M, Kuc K, Milewski JD, Nowacki A, Wojcik G, Kopczyk M (2000) J Power Sources 85:49
4. Devilliers D, Dinh Thi MT, Mahe E, Dauriac V, Lequeux N (2004) J Anal Chem 573:227
5. Hrussanova A, Mirkova L, Dobrev T (2001) Hydrometallurgy 60:199
6. Hrussanova A, Mirkova L, Dobrev T (2002) J Appl Electrochem 32:505
7. Hrussanova A, Mirkova L, Dobrev T, Vasilev S (2004) Hydrometallurgy 72:215
8. Hrussanova A, Mirkova L, Dobrev T, Vasilev S (2004) Hydrometallurgy 72:205
9. Koch DFA (1959) Aust J Chem 12:127
10. Koch DFA (1959) Electrochim Acta 1:32
11. Komaki A, Kawamura G, Mochizuki S (1982) Prog Batteries Solar Cells 4:167
12. Narasimham KC, Udupa HVK (1982) Proc Indian Natn Sci Acad 48A:346
13. Nguyen T, Atrens A (2007) submitted for publication to Hydrometallurgy
14. Nguyen YKT, Guresin N (2004) The effect of cobalt on the corrosion of lead anodes during copper electrowinning. Amira P705 project progress report, AJ Parker CRC for Hydrometallurgy, Brisbane, QLD
15. Nguyen T, Guresin G, Nicol M, Atrens A (2007) J Appl Electrochem accepted for publication DOI 10.1007/s 10800
16. Paleska I, Pruszkowska R, Kotowski J, Dziudzi A, Milewski JD, Kopczyk M, Czerwinski A (2003) J Power Sources 113:308
17. Panda B, Das SC, Panda RK (2004) Hydrometallurgy 72:149
18. Ramachandran P, Balakrishnan K (1990) Bull Ellectrochem 6:455
19. Rey M, Coheur P, Herbiet H (1938) Trans Amer Electrochem Soc 73:315
20. Yu P, O'Keefe JO (1999) J Electrochem Soc 146:1361
21. Yu P, O'Keefe TJ (1999) J Electrochem Soc 149:A558
22. Yu P, O'Keefe JO (2001) Polarization behaviour of new and used lead alloys in acid sulfate solutions, electrometallurgy 2001. Proceedings of the annual hydrometallurgical meeting, Toronto, Canada, Elsevier, p 129